AGU PUBLICATIONS

Geophysical Research Letters

RESEARCH LETTER
10.1002/2014GL061403

Key Points:
- The first entire concentric airglow image from the space
- Measurement of the spatial scale without assumption
- Propagation speed of the concentric structure was derived

Correspondence to:
Y. Akiya,
akiya@kugi.kyoto-u.ac.jp

Citation:
Akiya, Y., A. Saito, T. Sakanoi, Y. Hozumi, A. Yamazaki, Y. Otsuka, M. Nishioka, and T. Tsugawa (2014), First spaceborne observation of the entire concentric airglow structure caused by tropospheric disturbance, *Geophys. Res. Lett.*, *41*, 6943–6948, doi:10.1002/2014GL061403.

Received 5 AUG 2014
Accepted 1 SEP 2014
Accepted article online 3 SEP 2014
Published online 6 OCT 2014

First spaceborne observation of the entire concentric airglow structure caused by tropospheric disturbance

Y. Akiya[1], A. Saito[1], T. Sakanoi[2], Y. Hozumi[1], A. Yamazaki[3], Y. Otsuka[4], M. Nishioka[5], and T. Tsugawa[5]

[1]Graduate School of Science, Kyoto University, Kyoto, Japan, [2]Planetary Plasma and Atmospheric Research Center, Tohoku University, Sendai, Japan, [3]Institute of Space and Astronautical Science, Japan Aerospace Exploration Agency, Sagamihara, Japan, [4]Solar-Terrestrial Environmental Laboratory, Nagoya University, Nagoya, Japan, [5]National Institute of Information and Communications Technology, Koganei, Japan

Abstract Spaceborne imagers are able to observe the airglow structures with wide field of views regardless of the tropospheric condition that limits the observational time of the ground-based imagers. Concentric wave structures of the O_2 airglow in 762 nm wavelength were observed over North America on 1 June 2013 from the International Space Station. This was the first observation in which the entire image of the structure was captured from space, and its spatial scale size was determined to be 1200 km radius without assumptions. The apparent horizontal wavelength was 80 km, and the amplitude in the intensity was approximately 20% of the background intensity. The propagation velocity of the structure was derived as 125 ± 62 m/s and atmospheric gravity waves were estimated to be generated for 3.5 ± 1.7 h. Concentric structures observed in this event were interpreted to be generated by super cells that caused a tornado in its early phase.

1. Introduction

Airglow is the emission of light from atoms and molecules in the upper atmosphere. These atoms and molecules release their excess energy that is caused by the solar radiation in the daytime. Atmospheric gravity waves in the mesosphere and the lower thermosphere are studied via the observations of airglow by ground-based and spaceborne instruments [*Siskind and Sharp*, 1991; *Shepherd et al.*, 1993; *Hays et al.*, 1993; *Belyaev et al.*, 2006; *Makela et al.*, 2011; *Suzuki et al.*, 2013]. Variations in airglow emission are mainly caused by the variations of the number density and the temperature of atoms and molecules in the emission layer. A single all-sky imager with a field of view (FOV) of several hundred kilometers is insufficient for observing the entire wave structure, which may be larger than 1000 km [*Shiokawa et al.*, 1999].

The effects of tropospheric activity on airglow disturbances in the upper atmosphere have been previously studied. The circular structures of OH airglow disturbances, which have been interpreted to be caused by convective clouds, were partly observed by ground-based imager [*Yue et al.*, 2009]. Some concentric airglow structures have been related to thunder storm activities [*Taylor and Hapgood*, 1988; *Sentman et al.*, 2003; *Alexander et al.*, 2004]. A concentric gravity wave structure centered over a typhoon was observed by a ground-based imager in Japan [*Suzuki et al.*, 2007]. However, the entire structure of the concentric disturbance was not clarified from the ground-based observations, because of their narrow FOVs and restrictions due to weather conditions. Concentric structures of the airglow were observed mostly around tropospheric disturbances, which can be the sources of the atmospheric gravity waves (AGWs). The observation of these structures near AGW sources by ground-based imagers is difficult because their FOVs are often covered by clouds. The observations from the space can identify the sources of the concentric airglow structures over clouds.

The entire image of a concentric airglow structure was first observed on 1 June 2013 by the spectrographic imager on the International Space Station (ISS). The horizontal dimension of this concentric structure was 1200 km, which is larger than the FOV range of the ground-based imager.

2. Observation and Results

A concentric airglow emission event in the 762 nm wavelength was observed on 1 June 2013 by Visible and near Infrared Spectral Imager (VISI) of the ISS-IMAP mission (Ionosphere, Mesosphere, upper Atmosphere and Plasmasphere mapping mission from the ISS).

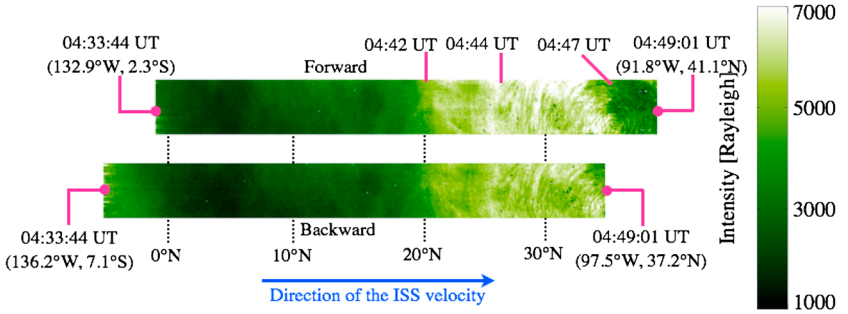

Figure 1. Images of the 762 nm observation by visible and near-infrared spectrographic imager (VISI). (top) The forward and (bottom) backward field of view (FOV) images. Images are plotted in the 1000–7000 R range. It is assumed that the emission layer altitude is 95 km. A concentric structure of the airglow emission is observed from 04:44 UT to 04:49 UT.

VISI was installed on July 2012, on the Exposure Facility of the Japanese Experiment Module on the ISS at an orbit of approximately 400 km. IMAP-VISI observes the airglow in the nadir direction on the nightside with two FOVs facing 45° in the forward and backward of the orbital direction [*Sakanoi et al.*, 2011]. Images taken by VISI are one-dimensional slit images along the perpendicular direction to the ISS trajectory. The FOVs of VISI are approximately 600 km wide at an altitude of 100 km perpendicular to the ISS orbit. The spatial resolution of VISI is approximately 10 km at the same altitude. The observational mode that records the peak and the background airglow emissions was used in this paper. Airglow emissions continuously observed by VISI were 630 nm O, 762 nm O_2 emission, and OH(8-3) band emission at approximately 730 nm [*Sakanoi et al.*, 2011]. These images were recorded at sampling intervals of 1.8 s. This sampling interval corresponds to a horizontal resolution of approximately 14 km along the ISS trajectory because the ISS moves approximately 8 km/s. For the direction perpendicular to the ISS trajectory, the spatial resolution of VISI at the altitude of 95 km is approximately 10 km.

An event observed over the North American continent on 1 June 2013 is the focus of this paper. The observational period was from 04:33:44 UT to 04:49:01 UT on 1 June 2013. Observational images of O_2 emission at 762 nm captured by VISI are shown in Figure 1. The 762 nm airglow emission from O_2 is at an altitude of approximately 95 km. Figures 1 (top) and 1 (bottom) are the observational images recorded by the forward and backward FOV of VISI, respectively. The horizontal axis in Figure 1 corresponds to the direction of the ISS velocity. The vertical axis is the direction of the slit of VISI. The ISS moved from left to right, as shown in Figure 1. The geographic coordinates shown in Figure 1 represent the positions of the center pixels of the images with the assumption that the emission layer centers at an altitude of 95 km. The green color in the figure indicates the 762 nm emission in the intensity range of 1000 R to 7000 R. The strongest emission in this observation was 7897 R. Emission in the region between the equator and 20°N was approximately 1000 R. The intensity observed by the backward FOV was weaker than that of the forward FOV. This difference may be caused by an inaccuracy in instrument calibration. Red lines in the figure indicate the positions of the data at the times shown in UT. The ISS was positioned 6.1°S, 135.6°W at the start and 38.1°N, 96.5°W at the end of this observation at an altitude of 410 km.

No light from the Moon was visible in this area. Reflection of the O_2 airglow emission by clouds at the 762 nm wavelength was absorbed by the Earth's atmosphere. Most of the emission of city lights were also absorbed by the Earth's atmosphere, although some in the image were strong and appeared as white pixels. Cosmic rays that struck the charge-coupled device (CCD) pixels also appear as white pixels in the observational image. Intense emissions of the O_2 airglow appeared between 20°N and 40°N. Intense emission was observed from 04:42 UT to 04:47 UT by the forward FOV of VISI. A wavy structure appeared at approximately 04:44 UT when the location of the center pixel of the forward FOV was at 29.9°N, 106.9°W. This wavy structure, observed for 5 min until the end of this observation at 04:49 UT, was concentric with the center near 35°N, 95°W. This structure was also observed in the backward FOV of VISI, although the entire image of the concentric structure was not captured by the backward FOV because the VISI observation ended at dawn.

The remainder of this paper mainly investigates the image of the forward FOV. High-pass filtered data with a cutoff wavelength of 700 km is shown in Figure 2. The geographic coordinates of Figure 2 are 110°W to 90°W longitude and 25°N to 45°N latitude. The center of concentric structure was estimated under the assumption that wavefronts are circular and that the structure has a single center. The estimated position

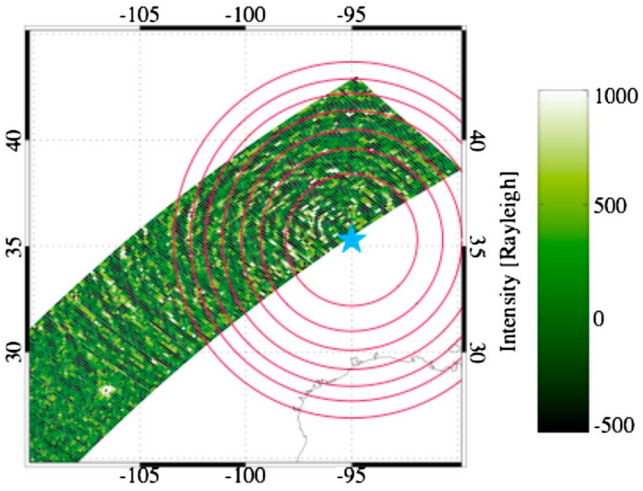

Figure 2. High-pass filtered observational data of visible and near-infrared spectrographic imager's (VISI) forward field of view (FOV). Data obtained near Oklahoma, United States, are plotted under the assumption that the emission layer exists at an altitude of 95 km. The unit of intensity is Rayleigh. Red lines in the figure indicate wavefronts in the concentric structure. The star in the figure indicates the estimated center of the structure.

of the center was at 35.3°N, 95.0°W which is represented by a star in Figure 2. Red circles indicate wavefronts from the estimated center; the smallest radius is 260 km. Some circular wavefronts were observed in a region closer than 260 km to the estimated center. The centers of these circular wavefronts appeared to differ; those inside the smallest circle in Figure 2 were in the region of 94°W to 96°W longitude and 34°N to 36°N latitude.

The high-pass filtered data on the line 35.3°N, 95.0°W, which is the estimated center, to 25°N, 108°W is shown in Figure 3. This line runs southwestward and is parallel to the ISS trajectory. The fluctuations from 0 km to 700 km correspond to the concentric structure in Figure 2. Spike of 2000 R around 300 km in Figure 3 corresponds to the city light. The average intensity of the peak-to-peak amplitude of the fluctuation was approximately 1000 R, which approximately represents a 20% fluctuation of the background airglow intensity. The amplitude of fluctuation does not significantly attenuate in the range of 0–1200 km, and the dominant wavelength of this structure was 40–80 km.

The propagation speed was estimated from the spatial difference between the forward and backward FOVs of VISI. The difference of 1 pixel size corresponds to 9.8 km at an altitude of 95 km. The interval of the observation by the forward and backward FOVs was 78 s at an altitude of 95 km. The difference of the concentric wavefronts between forward and backward FOVs was 1 or 0 pixels in the radial direction from the center. The propagation speed derived from this difference was 125 ± 62 m/s. Uncertainty of the propagation speed is caused by the spatial resolution of the VISI observation. The propagation speed derived from the difference between the two FOVs was 130–160 m/s, which is consistent with the phase velocity observed by previous studies [*Shiokawa et al.*, 1999; *Yue et al.*, 2013].

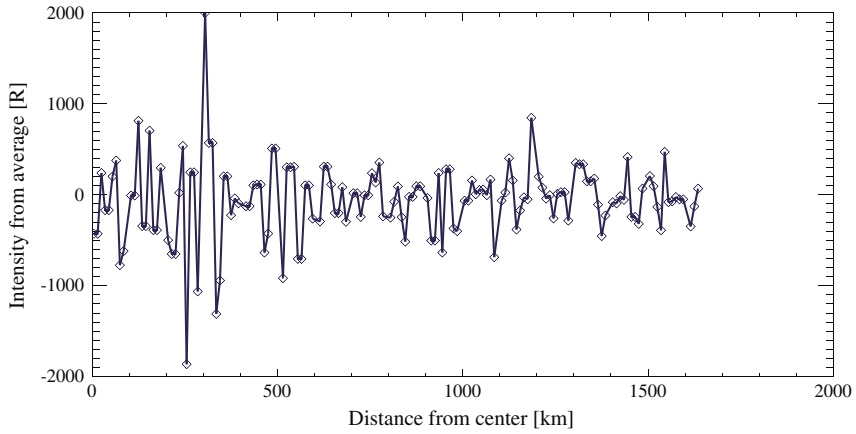

Figure 3. Variation of intensity from the center of the circular structure. The horizontal axis indicates the distance from the center of the concentric structure, and the vertical axis indicates fluctuation from the average intensity. The base line is taken from 35.3°N, 95.0°W to 25°N, 108°W parallel to the International Space Station (ISS) orbit.

3. Discussion

Concentric waves in the O_2 airglow emission were observed in the range of 1200 km radius from the center at approximately 04:40 UT on 1 June 2013. The width of the central region was 260 km in diameter with a dominant wavelength of 80 km. Its amplitude was 20% of the background intensity near the center and was nearly almost constant in a 1200 km radius from the center. The propagation speed of waves in the concentric structure was estimated to be 125 ± 62 m/s.

The duration time of the concentric structure was estimated from the propagation speed and the distance from the center to the edge of the structure. At a constant speed, the propagation time of waves from the center to the edge at 1200 km was estimated to be 3.5 ± 1.7 h. These results indicate that the concentric structure was created after 23:20 UT on 31 May which is the time evaluated from the slowest speed of propagation.

A decrease in intensity was not observed as waves of 80 km wavelength propagated to 1200 km. It is interpreted from this constant amplitude that waves were ducted near the emission layer. Dominant wavelength of 80 km could be determined by the ducted propagation mechanism. A numerical simulation based on the event observed in Brazil showed the duct propagation of AGW at an altitude of 90 km for a distance of 1000 km [*Vadas et al.*, 2009].

To identify the source of the concentric structure, the infrared observation of tropospheric clouds provided by the National Centers for Environmental Prediction/National Center for Atmospheric Research (NCEP/NCAR) was compared with that of the airglow emission by VISI. No clouds were observed before 23:00 UT on 31 May in the $3° \times 3°$ region near 35.3°N, 95.0°W which is the center of the concentric structure. A tornado occurred on 31 May from 23:03 UT to 23:43 UT near 35.5°N, 98.0°W as reported by the National Oceanic and Atmospheric Administration, approximately. This was 5 h prior to the observation of the concentric structure by VISI. Super cells that were observed as clouds with high-altitude tops existed for 5 h in the $3° \times 3°$ region near 35.5°N, 98.0°W after the tornado disappeared.

Observation of clouds at 04:00 UT on 1 June 2013 and the observation of the airglow by VISI are plotted in Figure 4. The range of this map is 25°N to 45°N latitude and 110°W to 90°W longitude, which is the same as that shown in Figure 2. The cloud is plotted according to VISI observation in Figure 4 (top). Color in the figure indicates the temperature of the cloud top in 203–313 K range. VISI observation is plotted in green at the position under the assumption that the emission layer existed at an altitude of 95 km. The center of the concentric structure is represented by the blue star in the figure, and wavefronts are represented by red circles in Figure 4 (bottom). The intervals of these circles were 80–100 km in the radial direction, which corresponds to the dominant wavelength of this concentric structure. Clouds with top temperatures of approximately 215 K were observed at approximately 35.3°N, 95.0°W, which is the center position of the concentric structure. Many circular wavefronts of the airglow were observed inside the central region, which correspond to the inside of the smallest circle in Figure 4 (bottom). Multiple centers of circular waves appeared to exist inside of the central region. Ripples of the airglow intensity variation can be generated when multiple sources exist nearby [*Vadas et al.*, 2012]. Several clouds with high-altitude cloud tops under the region of multiple circular wavefronts of the airglow were observed by VISI. The sources of these circular wavefronts appeared to exist inside a diameter of 260 km from the center. Super cells, which correspond to clouds with high-altitude cloud tops near 35.3°N, 95.0°W, are believed to be the source of AGWs that generate the concentric structure in the airglow emission outside the region. The dominant 80 km wavelength in this concentric structure is consistent with that of the airglow structure caused by thunder storms [*Vadas et al.*, 2012; *Yue et al.*, 2013].

Global positioning system-total electron content (GPS-TEC) observed by ground-based receivers were investigated to study the altitude range in which AGWs propagated in the vertical direction. Data of ground-based GPS receivers in North America were used. The horizontal structure of TEC perturbation was studied by 20 min detrended data of the DRAWING-TEC project (http://seg-web.nict.go.jp/GPS/DRAWING-TEC/) of Japan's National Institute of Information and Communications Technology (NICT). Concentric structures in TEC were clearly observed from 23:30 UT on 31 May 2013 to 01:30 UT on 1 June 2013. The center of the TEC concentric structure was near 35.5°N, 98.0°W, which is the position that the tornado existed from 23:03 UT to 23:53 UT on 31 May. The radius of the TEC concentric structure was 1500 km at 01:00 UT, which was larger than that of the concentric structure observed by VISI. The amplitude of TEC

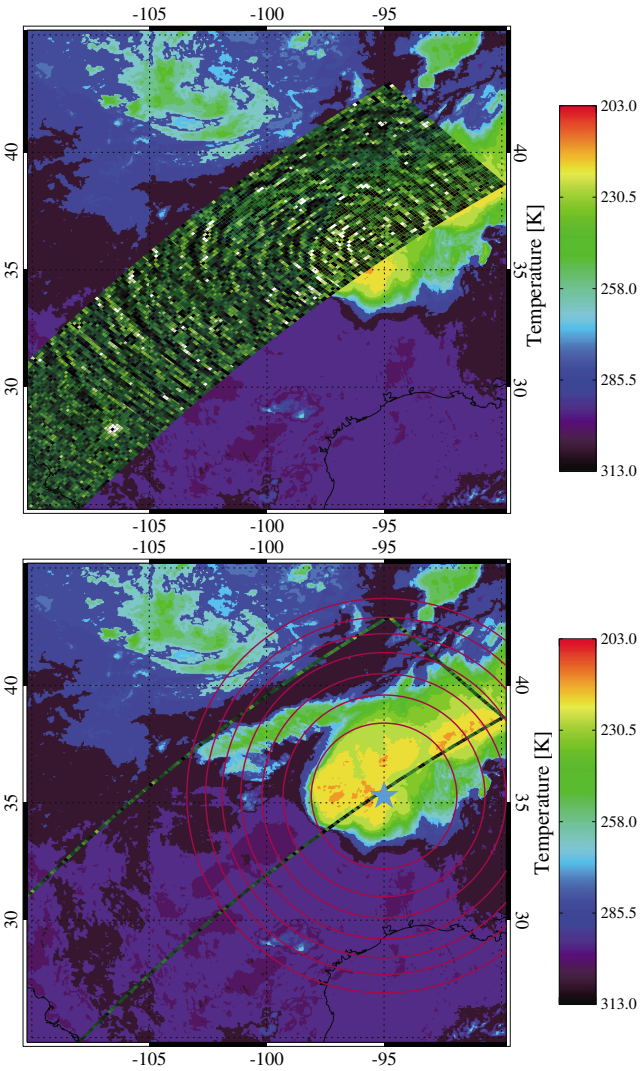

Figure 4. (top and bottom) Infrared image of clouds recorded at 04:00 UT on 1 June 2013. Temperature of clouds is indicated by contour. The frame of the region of visible and near-infrared spectrographic imager (VISI) observation is shown as a green rectangle. Red circles indicate wavefronts observed by VISI.

perturbation was large in the northeast direction and was small in the northwest. The dominant wavelength of the TEC concentric structure was 150 km, which is longer than that in the airglow observation. The propagation speed was estimated to be 160–180 m/s, which is faster than that of the wavefronts in the airglow concentric structure observed by VISI. Enhancement of TEC was caused by a geomagnetic storm from 01:30 UT on 1 June, with a minimum value of the *Dst* index −119 nT at 09:00 UT on 1 June. TEC concentric structures were not clearly observed after 01:30 UT. It is interpreted that AGWs generated in the troposphere propagated in the 300 km altitude and generated the concentric structure in TEC. AGWs that generated the TEC concentric structure differed from those that generated the airglow concentric structure because the wavelength and propagating velocity differed. This result is consistent with the AGW theory that TEC concentric structures with longer wavelengths propagate faster than airglow concentric structures with shorter wavelengths.

The start time of the airglow concentric structure was estimated between 23:20 UT on 31 May and 03:00 UT on 1 June, which was calculated from the propagation speed of AGWs in the concentric structure. If the airglow concentric structure had started before 01:30 UT, the concentric structure of the airglow and that of the TEC would have simultaneously existed. The dominant wavelength of the airglow concentric structure was 80 km, which is shorter than that of the TEC concentric structure. Difference of the dominant wavelengths between TEC and airglow concentric structures could be caused by the difference of the generation and propagation mechanisms. Furthermore, the TEC concentric structure produced by a different tornado endured for 7 h over North America [*Nishioka et al.*, 2013].

4. Conclusion

The entire structure of a concentric airglow emission in the mesosphere was first observed by the ISS/IMAP-VISI. An image of the O_2 airglow emission obtained at the 762 nm wavelength was used in this study. A concentric structure was reported in the observation of 1 June 2013. The distance from the center to the edge of this concentric emission was approximately 1200 km, and the dominant horizontal wavelength was 80 km. The average amplitude near the source was 1000 R, which is 20% of the background. Attenuation was not apparent in this event. The center of the concentric structure was near the high-altitude top clouds that existed at the time of the VISI observation. Multiple wavefronts were observed near the center of the concentric structure. The duration time of the AGW source was estimated from the entire

concentric airglow structure. The concentric structure without attenuation was estimated to be made by horizontal propagation of AGWs for 3.5 h in the radial direction from the center. Multiple wavefronts near the center were appeared to be generated from different points in highly convective clouds. It is supposed that the concentric structure observed in this event was created from highly convective clouds and that AGWs horizontally propagated with little damping.

This is the first complete observation of the concentric airglow structure from the space. It was able to derive horizontal propagation distance, wavelength, and velocity. This observation had shown that a single perturbation in the troposphere can generate atmospheric gravity waves which propagate to a distance of more than 1000 km in the lower thermosphere.

Acknowledgments

Data to support this article are from the Ionosphere, Mesosphere, upper Atmosphere, and Plasmasphere mapping mission from the ISS (ISS-IMAP mission), National Centers for Environmental Prediction/National Center for Atmospheric Research (NCEP/NCAR), and DRAWING-TEC of National Institute of Information and Communications Technology (NICT). We would like to thank all the members of the IMAP mission for their support in developing VISI. We also thank Takeyama, Kanai, and Obuchi for their contribution in manufacturing the optical system of VISI. In addition, we thank Tanaka and other members of Meisei Corporation for their help in developing the electronics.

The Editor thanks Michael Kelley and an anonymous reviewer for their assistance in evaluating this paper.

References

Alexander, M. J., P. T. May, and J. H. Beres (2004), Gravity waves generated by convection in the Darwin area during the Darwin area wave experiment, *J. Geophys. Res.*, *109*, D20S04, doi:10.1029/2004JD004729.

Belyaev, A. N., V. V. Alpatov, E. Blanc, and V. E. Melnikov (2006), Space-based observations of O_2 A (0,0) band emission near the solar terminator and their interpretation, *Adv. Space Res.*, *38*(11), 2366–2373.

Hays, P. B., V. J. Abreu, M. E. Dobbs, D. A. Gell, H. J. Grassi, and W. R. Skinner (1993), The high-resolution doppler imager on the upper atmosphere research satellite, *J. Geophys. Res.*, *98*, 10,713–10,723.

Makela, J. J., et al. (2011), Imaging and modeling the ionospheric airglow response over Hawaii to the tsunami generated by the Tohoku earthquake of 11 March 2011, *Geophys. Res. Lett.*, *38*, L00G02, doi:10.1029/2011GL047860.

Nishioka, M., T. Tsugawa, M. Kubota, and M. Ishii (2013), Concentric waves and short-period oscillations observed in the ionosphere after the 2013 Moore EF5 tornado, *Geophys. Res. Lett.*, *40*, 5581–5586, doi:10.1002/2013GL057963.

Sakanoi, T., Y. Akiya, A. Yamazaki, Y. Otsuka, A. Saito, and I. Yoshikawa (2011), Imaging observation of the Earth's mesosphere, thermosphere and ionosphere by VISI of ISS-IMAP on the international space station, *IEEE Trans. Fundam. Mater.*, *131*(12), 983–988.

Sentman, D. D., E. M. Wescott, R. H. Picard, J. R. Winick, H. C. Stenbaek-Nielsen, E. M. Dewan, D. R. Moudry, F. T. São Sabbas, M. J. Heavner, and J. Morrill (2003), Simultaneous observations of mesospheric gravity waves and sprites generated by a midwestern thunderstorm, *J. Atmos. Sol. Terr. Phys.*, *65*, 537–550.

Shepherd, G. G., et al. (1993), WINDII, the wind imaging interferometer on the upper atmosphere research satellite, *J. Geophys. Res*, *98*, 10,725–10,750.

Shiokawa, K., Y. Kato, M. Satoh, M. K. Ejiri, T. Ogawa, T. Nakamura, T. Tsuda, and R. H. Wiens (1999), Development of optical mesosphere thermosphere imagers (OMTI), *Earth Planets Space*, *51*, 887–896.

Siskind, D. E., and W. E. Sharp (1991), A comparison of measurements of the oxygen nightglow and atomic oxygen in the lower thermosphere, *Planet. Space Sci.*, *39*(4), 627–639.

Suzuki, S., K. Shiokawa, Y. Otsuka, T. Ogawa, K. Nakamura, and T. Nakamura (2007), A concentric gravity wave structure in the mesospheric airglow images, *J. Geophys. Res.*, *112*, D02102, doi:10.1029/2005JD006558.

Suzuki, S., K. Shiokawa, Y. Otsuka, S. Kawamura, and Y. Murayama (2013), Evidence of gravity wave ducting in the mesopause region from airglow network observations, *Geophys. Res. Lett.*, *40*, 601–605, doi:10.1029/2012GL054605.

Taylor, M. J., and M. A. Hapgood (1988), Identification of a thunderstorm as a source of short period gravity waves in the upper atmospheric nightglow emissions, *Planet. Space Sci.*, *36*(10), 975–985.

Vadas, S., J. Yue, and Nakamura T. (2012), Mesospheric concentric gravity waves generated by multiple convective storms over the North American Great Plain, *J. Geophys. Res.*, *117*, D07113, doi:10.1029/2011JD017025.

Vadas, S. L., M. J. Taylor, P.-D. Pautet, P. A. Stamus, D. C. Fritts, H.-L. Liu, F. T. São Sabbas, V. T. Rampinelli, P. Batista, and H. Takahashi (2009), Convection: The likely source of the medium-scale gravity waves observed in the OH airglow layer near Brasilia, Brazil, during the SpreadFEx campaign, *Ann. Geophys.*, *27*, 231–259.

Yue, J., S. L. Vadas, C.-Y. She, T. Nakamura, S. C. Reising, H.-L. Liu, P. Stamus, D. A. Krueger, W. Lyons, and T. Li (2009), Concentric gravity waves in the mesosphere generated by deep convective plumes in the lower atmosphere near Fort Collins, Colorado, *J. Geophys. Res.*, *114*, D06104, doi:10.1029/2008JD011244.

Yue, J., L. Hoffmann, and M. Joan Alexander (2013), Simultaneous observations of convective gravity waves from a ground-based airglow imager and the AIRS satellite experiment, *J. Geophys. Res. Atmos.*, *118*, 3178–3191, doi:10.1002/jgrd.50341.